Conformation, Orientation, and Adsorption Kinetics of Dermaseptin B2 onto Synthetic Supports at Aqueous/Solid Interface

S. Noinville,* F. Bruston,† C. El Amri,* D. Baron,* and P. Nicolas†
*Laboratoire de Dynamique, Interactions et Réactivité, Centre National de la Recherche Scientifique-Université Paris, 94320 Thiais, France; and †Laboratoire de Bioactivation des Peptides, Institut Jacques Monod, 75251 Paris cedex 5, France

ABSTRACT The antimicrobial activity of cationic amphipathic peptides is due mainly to the adsorption of peptides onto target membranes, which can be modulated by such physicochemical parameters as charge and hydrophobicity. We investigated the structure of dermaseptin B2 (Drs B2) at the aqueous/synthetic solid support interface and its adsorption kinetics using attenuated total reflection Fourier transform infrared spectroscopy and surface plasmon resonance. We determined the conformation and affinity of Drs B2 adsorbed onto negatively charged (silica or dextran) and hydrophobic supports. Synthetic supports of differing hydrophobicity were obtained by modifying silica or gold with ω-functionalized alkylsilanes (bromo, vinyl, phenyl, methyl) or alkylthiols. The peptide molecules adsorbed onto negatively charged supports mostly had a β-type conformation. In contrast, a monolayer of Drs B2, mainly in the α-helical conformation, was adsorbed irreversibly onto the hydrophobic synthetic supports. The conformational changes during formation of the adsorbed monolayer were monitored by two-dimensional Fourier transform infrared spectroscopy correlation; they showed the influence of peptide-peptide interactions on α-helix folding on the most hydrophobic support. The orientation of the α-helical Drs B2 with respect to the hydrophobic support was determined by polarized attenuated total reflection; it was around 15 $\pm$ 5°. This orientation was confirmed and illustrated by a molecular dynamics study. These combined data demonstrate that specific chemical environments influence the structure of Drs B2, which could explain the many functions of antimicrobial peptides.

INTRODUCTION

The dermaseptins (Drs) are antimicrobial peptides that have been isolated from the skin secretions of the arboreal South American frogs *Phyllomedusa sauvagii* (Drs S) (Mor et al., 1994b), *P. oreades* and *distincta* (Brand et al., 2002), and *P. bicolor* (Drs B) (Charpentier et al., 1998; Daly et al., 1992; Mor et al., 1994a; Strahilevitz et al., 1994). These peptides are 24–34 amino acid residues long with a conserved tryptophan at position 3, and have a net positive charge (Lys-rich). Dermaseptin B2 (Drs B2) is the most abundant and active of the Drs B peptides. Prediction methods and preliminary circular dichroism (CD) experiments have shown that it has no definite structure in water, but contains 45–90% helix in structure-promoting solvents such as trifluoroethanol (data not shown). Like several other cationic antimicrobial peptides (Fleury et al., 1996; Park et al., 2001), Drs B2 is believed to adopt an amphipathic helical structure when bound to membranes, with one external surface being positively charged and the other hydrophobic (Nicolas and Mor, 1995). Peptide adsorption is a key phenomenon during the interaction with membranes that could promote changes in membrane bilayer curvature (Matsuzaki et al., 1998) or membrane micellisation by a detergent-like effect (Shai, 1999), but could also involve competing conformational states, or aggregation of the adsorbed peptides that may influence their antimicrobial activities. The effects of peptide hydrophobicity on their antimicrobial activities have been studied by residue substitution (Feder et al., 2000; Lee et al., 2002; Wade et al., 2000), or using analog peptides (Kumary and Nagaraj, 2001; Kustanovich et al., 2002; Kwon et al., 1998), as well as on their ability to form α-helices (Kustanovich et al., 2002).

The immobilization of active peptides or proteins onto polymer materials to improve their biocompatibility is a major focus in different applications such as affinity separation, diagnostics, proteomics, and cell culture technologies (Long et al., 2002). The major concern is retention of structure and biological function of the immobilized peptides or proteins. More generally, the structure of the adsorbed layer governs its biochemical function, whether that be enzymatic or antimicrobial activity or receptor-ligand binding (Bower et al., 1995; Harvey et al., 1995; Hlady and Buijs, 1996; Norde, 2000). It has been shown at the air/water interface that the secondary structure of the amphipathic peptides is much more influenced on the periodicity of the hydrophobic and hydrophilic residues in the peptide sequence than on the helical propensity of a particular amino acid (Maget-Dana, 1999). In contrast with the usual unfolding of proteins adsorbed on hydrophobic supports, amphipathic peptides such as Drs B2 fold into α-helical structure in a hydrophobic environment. The immobilized peptide on solid hydrophobic supports should adopt a more folded state because the planar environment restricts the conformational degrees of freedom. Moreover, the hydrophobicity or the polarity of the adsorbent surface may also influence the conformation of adsorbed amphipathic peptides. Understanding at a molecular level peptide structure on

Submitted November 29, 2002, and accepted for publication April 16, 2003.

Address reprint requests to Dr. S. Noinville, Laboratoire de Dynamique, Interactions et Réactivité, CNRS, 2 rue Henri Dunant, 94320 Thiais, France. Tel.: 00-33-149-781-292; Fax: 00-33-149-781-18; E-mail: sylvie.noinville@glvt-cnrs.fr.

0006-3495/03/08/1196/11 $2.00

surfaces depending on their hydrophobic or polar character should optimize the functional properties of peptide coatings.

We have therefore investigated the structural changes and kinetics of the adsorption of Drs B2 so as to understand its molecular interactions with solid surfaces with various hydrophobicities. We used appropriate techniques sensitive enough to detect the submonolayer of peptides under controlled conditions of mass transport. These were attenuated total reflection Fourier transform infrared (ATR-FTIR) spectroscopy under stationary conditions and surface plasmon resonance (SPR) spectroscopy for continuous flow. These two techniques allowed us to work with low peptide concentrations in the range of the antimicrobial activity of Drs B2 (1 μM) and at a physiological pH.

The present paper describes the adsorption of Drs B2 onto negatively charged hydrophilic supports and hydrophobic supports. The characteristics of the adsorbent surfaces used for ATR and SPR were also well defined. Self-assembled organic monolayers (SAMs) are excellent for modifying the surface properties at a molecular level. SAMs can be prepared from solutions containing alkylsilanes or alkylthiols to modify silica (ATR) or gold (SPR) surfaces, giving hydrophobic supports (Wasserman et al., 1989; Whitesides and Laibinis, 1990). We also varied the end group of the trichlorosilyl surfactant, using an amine, vinyl, bromo, or phenyl group to provide other surfaces of differing hydrophobicity. The negatively charged hydrophilic supports were the bare silica layer for the ATR element and a dextran matrix grafted onto gold for the SPR experiment.

FTIR spectroscopy is increasingly used to obtain information on the conformation of proteins or peptides in aqueous or organic media, or attached to lipid bilayers and surfactant micelles (Castano et al., 1999; Goormaghtigh and Ruysschaert, 1990; Lewis et al., 1999). The ATR-FTIR technique is well suited to determine secondary structure of peptides or proteins adsorbed on solid supports. This method can also be used to quantify their adsorbed amount at the aqueous/sorbent interface (Noinville et al., 2002). The infrared absorption amide I' band in peptides or proteins corresponds to the C=O stretching vibrational mode of the CON^2H amide groups, whose frequency depends strongly on the local environment. Perturbation-dependent structural changes in proteins have been studied by several techniques, including 2D-infrared correlation spectroscopy. The 2D correlation studies have added greater confidence to the understanding of the conformational changes that proteins undergo in response to changes in various physical-chemical conditions, such as temperature, pressure, and $H/^2H$ exchange (Fabian et al., 1999; Meskers et al., 1999; Smeller and Heremans, 1999). 2D correlation analysis has been used to monitor adsorption-induced changes in a protein (Czarnik-Matusewicz et al., 2000).

Surface plasmon resonance allows the kinetics of the interactions between a peptide and the adsorbent surface to be monitored in real time (Mrksich et al., 1995). An SPR shift during the adsorption gives information about the concentration of peptide at the adsorbent surface. The use of optical biosensors to monitor the nonspecific adsorption of a soluble protein or peptide to a synthetic surface has been reviewed (Hall, 2001; Ramsden, 1998).

Our ATR-FTIR spectroscopy and SPR investigations revealed the structure of the adsorbed Drs B2 and the amount adsorbed, as well as the distribution of the peptide conformational states and their orientations relative to the solid support. We compared the structure of the Drs B2 adsorbed onto the most hydrophobic support with molecular dynamics simulation illustrating and confirming the orientation of the Drs B2. Little has been published to date on modeling the structure of an adsorbed biomolecule in contact with a solid surface. An approach using an AMBER force field to compute interaction energies in a protein/synthetic polymer system has been proposed and showed the preferred orientation of the protein studied at the interface (Noinville et al., 1995).

MATERIALS AND METHODS

Chemicals

Resin and Fmoc amino acids were from PerSeptive Biosystems Ltd. (Voisins-le-Bretonneux, France). Chloroform, dichloromethane, carbon tetrachloride, trifluoroacetic acid (TFA), trifluoroethanol, dimethylformamide and other reagents used for peptide synthesis were purchased from SDS (Peypin, France). Hexadecane (SDS) was passed through alumina molecular sieves to remove polar contaminants. Octadecyltrichlorosilane (Roth, Lauterbourg, France) was distilled under vacuum before use. Undecenyltrichlorosilane ($CH_2 = CH\text{-}(CH_2)_9SiCl_3$) was synthesized from 10-undecen-1-ol (Lancaster, Bischheim, France) according to Wasserman (Wasserman et al., 1989). 1-bromo-11(trichlorosylil)undecane ($Br\text{-}(CH_2)_{11}\text{-}SiCl_3$) was obtained by hydrosylilation of 1-bromo-10-undecene (45% yield) and purified by distillation under vacuum (Balachander and Sukenik, 1990). 1-bromo-10-undecene was synthesized from 10-undecen-1-ol as described by Schweizer et al. (1969). 1-Phenyl-17(trichlorosylil)heptadecane ($C_6H_5\text{-}(CH_2)_{17}\text{-}SiCl_3$) was synthesized in 50% yield by radical addition of trichlorosilane acid (Acras, France) to 1-phenyl-16-heptadecene $C_6H_5\text{-}(CH_2)_{15}\text{-}CH = CH_2$ according to Losset et al. (1991). The catalyst H_2PtCl_6 was purchased from Acras. The alkenes and final products were isolated by vacuum distillation as colorless liquids and their purity was checked by ^{1}H-NMR spectroscopy in C^2HCl_3 (Bruker 200 MHz).

Solid phase peptide synthesis

Dermaseptin B2 (3180 Da) from *Phyllomedusa bicolor* (sequence: GLWSKIKEVGKEAAKAAAKAAGKAALGAVSEAV-NH_2) was prepared by stepwise solid-phase synthesis using Fmoc polyamide active ester chemistry on a Milligen 9050 Pep Synthesizer Milli Gen. PAL-PEG-PS (peptide amide linker polyethyleneglycol polystryrene copolymer) resin was used for carboxamidation of the carboxyterminal residue of the peptide. Lysine and tryptophan side chains were protected with *tert*-butyloxycarbonyl (*t*-Boc), glutamic acid side chains with O-*tert*-butyl ester (O*t*Bu), and serine side chains with O-*tert*-butyl ether (*t*Bu). Synthesis was carried out using a triple-coupling protocol. Nα-Fmoc-amino acids (4.4 molar excess) were coupled for 30–60 min with 0.23 M diisopropylcarbodiimide in a mixture of dimethylformamide and dichloromethane (60:40, v/v). Acylation was

checked after each coupling step by the Kaiser test. Cleavage of the peptidyl resins and side chain deprotection was carried out at a concentration of 40 mg of peptidyl resin in 15 mL of 95% TFA, 2.5% triisopropylsilane, and 2.5% water for 2 h at room temperature. The resin was removed by filtration and the crude peptide was precipitated with ether at 20°C. The peptide was recovered by centrifugation at 5000 g for 10 min, washed three times with cold ether, dried under nitrogen, dissolved in 10% acetic acid, and lyophilized. The lyophilized crude peptide was purified by preparative reverse-phase high-performance liquid chromatography on a C18 reverse-phase column (N5C18-25M, Interchrom) eluted at 4 mL/min with a 40–60% linear gradient of acetonitrile in 0.07% TFA in water. The homogeneity of the synthetic peptide was assessed by analytical high-performance liquid chromatography on a Lichrosorb C18 column (5 μm, 4.6 $\times$ 250 mm) eluted at 0.75 mL/min with a linear gradient of acetonitrile/0.07% TFA in 0.1% trifluoroacetic acid/water. Peptide was detected by absorption at 280 nm. The purity was verified by Maldi-Tof mass spectrometry.

Treatment of ATR silicon crystals

All the ATR silicon crystals were cleaned to oxidize the surface and remove any organic contaminants. The ATR crystals were covered with a thin layer of silica and immersed in trichlorosilane (5 mM in hexadecane/CCl_4 (70:30)) for 1–3 h, rinsed with chloroform, and dried under a nitrogen stream. Self-assembled monolayers were formed on the silicon crystals according to Wasserman et al. (1989). The contact angles of water droplets on the surfaces modified by the SAMs (Table 1) were measured with a Krüss G10 goniometer. The chemically modified surfaces used to study Drs B2 adsorption were classified according to their hydrophobicity: Si/SiOH (bare crystal support) < [amine] < [bromo] < [vinyl] < [phenyl] < [methyl].

FTIR measurements

The trifluoroacetate (CF_3COO^-) peptide counterions were exchanged for chloride ions by lyophilizing the peptide two times in 80 mM HCl. This eliminated the strong contribution of the antisymmetric stretching band of the carboxylate groups of CF_3COO^- at 1673 cm^{-1} to the peptide amide I′ band (Laczko et al., 1992). The lyophilized Drs B2 was dissolved in deuterated phosphate buffer (55 mM $Na_2{}^2H$ PO4) in ^2H_2O adjusted to p^{2}H 7.5 with ^{2}HCl at a final Drs B2 concentration of 0.3–3 μM.

The ATR-FTIR spectra of adsorbed peptide were recorded on a Nicolet Magna IR 850 spectrometer equipped with a MCT detector. For each spectrum, 300 co-added scans, at a resolution of 4 cm^{-1} with one level of zero filling and a boxcar apodization were collected. The reference spectrum was obtained after filling the liquid-ATR cell with deuterated phosphate buffer (p^{2}H 7.5). Spectra were collected every 5 min for the first 30 min, then every 15 min under a continuous purge of residual water vapor. The same procedure was used after filling the cell with the dermaseptin solution. The ATR spectra of the adsorbed Drs B2 were obtained by subtracting the spectrum of the buffer solutions from the spectrum of the dermaseptin solutions at the same time of contact with the ATR crystal to remove the infrared absorption bands of buffer and water vapor. The cell was emptied and rinsed with deuterated buffer at the adsorption plateau. Since the peptide concentration was <3 μM, 99% of the infrared signals came from the peptide adsorbed at the aqueous/support interface, with <1% from the peptide molecules in solution. The peptide amide hydrogens of Drs B2 were fully deuterated after 20 min of incubation in deuterated buffer at p^{2}H 7.5. The spectral range of conformational interest, the amide I′ band around 1590–1710 cm^{-1}, was analyzed by Fourier self-deconvolution (FSD) using Omnic software (Nicolet, USA). The integrated absorbance of the amide I′ band was used to quantify the amount of peptide adsorbed onto the monolayers (Noinville et al., 2002). Since the refractive index of the buffer was not significantly changed by the low concentrations of peptide used, the surface density (Γ') was determined on line during adsorption.

A gold wire KRS-5 polarizer was used to measure the parallel and perpendicular polarized ATR spectra of Drs B2 adsorbed onto the hydrophobic support [methyl]. Experiments were performed in triplicate, and the reported data are averaged values. The spectra of ^2H_2O in contact with the hydrophobic support were recorded for each polarization and subtracted from the respective spectra of the monolayer of Drs B2 rinsed with pure ^2H_2O. Spectral decomposition was performed using Origin 5.0 software before evaluating the absorption intensities at the selected vibrational modes. The dichroic ratio of the α-helix component band was determined by calculating the ratio of measured absorption intensities for light polarized parallel and perpendicular to the plane of incidence.

2D FTIR correlation analysis

The 2D analysis of the ATR spectra was performed from time-dependent ATR-FTIR spectra in the spectral range 1590–1710 cm^{-1} by the procedure developed by Noda et al. (Noda, 1990). The synchronous 2D-correlation spectrum (S-map) displayed auto peaks on the diagonal reflecting IR component bands that varied with time. Crosspeaks were observed for component bands having correlated dynamic behaviors. The asynchronous 2D-correlation spectrum (A-map) lacked auto peaks and had asymmetric crosspeaks that revealed the out-of-phase behavior of two component bands. The crosspeaks at wavenumbers (ν_1, ν_2) with the same sign in the S- and A-maps indicated that a spectral change of the IR signal at the ordinate ν_2 preceded that of the IR signal at the abscissa ν_1 (Lecomte et al., 2001).

All ATR spectra were normalized to an optical path of 50 μm to obtain spectra independent of the penetration depth. The baseline, a two-point line between 1590 and 1710 cm^{-1}, was subtracted from the ATR-corrected spectra and they were normalized before 2D correlation analysis. The normalization factor was the value of integral intensities over the spectral range studied. The normalization procedure has been described previously (Czarnik-Matusewicz et al., 2000). The time-dependent changes in the infrared signals, corresponding to the amide I′ infrared absorption bands, reflected the changes in Drs B2 structure caused by adsorption onto the SAM.

Determination of orientation from the polarized ATR spectra

Polarized ATR spectroscopy is widely used to estimate the molecular order of systems axially symmetrical with respect to the normal ATR crystal surface (Axelsen and Citra, 1996). We used the angular convention of Citra and Axelsen to determine the molecular order S_m of Drs B2 adsorbed at the ^2H_2O/hydrophobic interface from the transition moment of the selected amide I′ band based upon the relationship (Citra and Axelsen, 1996):

$$S_m = \frac{E_x^2 - R \times E_y^2 + E_z^2}{P_2(\cos\Theta) \times (E_x^2 - R.E_y^2 - 2 \times E_z^2)} = P_2(\cos\gamma) \quad (1)$$

TABLE 1 Plateau densities of Drs B2 adsorbed onto chemically modified surfaces classified according to increasing hydrophobicity

Planar surface	Bare silica	[Amino]	[Bromo]	[Phenyl]	[Vinyl]	[Methyl]
Γ_{limit} (molecule/nm^2)	0.245	0.035	0.175	0.12	0.145	0.145
Advancing contact angle	<8°	62 ± 2°	83 ± 2°	92 ± 2°	96 ± 2°	110 ± 2°
Receding contact angle		45 ± 3°	75 ± 3°	82 ± 3°	87 ± 3°	96 ± 3°

where R is the experimental dichroic ratio, Θ is the angle between the transition moment of the α-helix vibrational mode and the α-helix long axis, γ is the angle between the molecular axis and the z axis (normal to the ATR crystal surface), $P_2(\cos\Theta)$ corresponds to the second order of Legendre polynomial equal to $(3\cos^2\Theta - 1)/2$, and E_x^2, E_y^2, and E_z^2 are the mean squared amplitudes of the electric field of the evanescent wave at the ^2H_2O/silicon interface. The value of angle Θ is needed to determine the orientation. We used $\Theta = 43°$ for the amide I′ vibration. This value was determined experimentally by measuring the dichroism of a model α-helical polypeptide at the ^2H_2O/hydrophobic surface (Citra and Axelsen, 1996). However, this value for the α-helix infrared band could be affected by deviations from the regular α-helical geometry depending on the H-bonding strength (Marsh et al., 2000). The amplitudes of the electric field at mid-IR radiation do not decay significantly along the z axis in the order of the molecular dimension of the silane coating (Axelsen and Citra, 1996). The electric field amplitudes were therefore calculated for a two-phase system from the relationships given by Harrick (1967) with refractive index values of 3.43 for the semiinfinite bulk phase silicon and 1.32 for the ^2H_2O.

Surface plasmon resonance

SPR experiments were carried out on a Biacore 2000 (Biacore, Uppsala, Sweden) using HPA and CM5 sensor chips. The HPA sensor chip was composed of octadecanethiol covalently bonded to the gold surface to give a hydrophobic monolayer (Cooper et al., 1998). The CM5 sensor chip was composed of a carboxymethylated dextran matrix that yielded a hydrophilic, negatively charged surface (COO^- groups). All experiments were performed at 25°C in running phosphate buffer (1 mM, NaH_2PO_4/Na_2HPO_4, pH 7.4) that had been degassed and passed through a 0.22-μm filter. Drs B2 was diluted to 1μM to 50 μM. Layouts were obtained at flow rate of 10 μL/min to avoid limitation by mass transport. Kinetics were measured with a 3-min adsorption step followed by a 3-min desorption step. The HPA surface was regenerated by repeated injections of 40 mM *n*-octyl-D-glucopyranoside at 10 μL/min until the initial baseline was reached. The CM5 surface was regenerated reproducibly by injecting 10 mM NaOH (50 μL, 100 μL/min). Analysis of SPR profiles was performed using BIAevaluation 3.1 software taking part of Biacore instrument.

Molecular simulation

The initial structure of Drs B2 was constructed as an ideal α-helix at pH 7. The six lysine side chains and Gly-1 end group were protonated (NH_3^+), and the three glutamate side chains were deprotonated (COO^-). The net charge of the peptide (+4) was neutralized by 4 Cl^- ions positioned along the Cα-N axis for Gly-1, and the Cε-N axis for Lys-7, Lys-19, and Lys-29, at 3.5 Å of N. This configuration was chosen to optimize the spatial distribution of the positive and negative charges along the helix axis.

The hydrophobic planar surface was generated using a rectangular set of 84 ethane molecules with their C-C axes perpendicular to the xy plane along the z direction, with 12 molecules stacked in the x direction, and seven along the y direction. The distance between the ethyl carbons of two adjacent molecules was 5 Å. The resulting hydrophobic surface was 57.5 Å long (x axis), 26 Å wide (y axis), and 1.5 Å thick (z axis) (see an illustration on Fig. 8 presented in Results and Discussion). The peptide helix axis was placed parallel to the x axis of the hydrophobic support to optimize the distance between Ala-28-C_β of the peptide and the hydrophobic surface. The χ_1 of Trp-3 side chain was constrained in a g^- conformation, to ensure a convenient distance between the hydrophobic surface and the peptide. The peptide was positioned with the nearest hydrogen atom (Trp-3-Hε1) at 3 Å from the nearest ethyl carbon atom of the hydrophobic plate.

Molecular dynamics were simulated in explicit water (dielectric constant set at 80, and cutoff of 12 Å) with periodic boundary conditions using the Discover 3 software in the Insight II 95.0 software package (Accelrys, formerly Molecular Simulations, San Diego, CA). The CVFF force field was applied with a harmonic potential for bond lengths without any cross terms (Hagler et al., 1979). The box size of the simulated systems (free Drs B2 or Drs B2 adsorbed to the hydrophobic surface) was 29 × 64 × 33 Å. These systems were minimized before simulation. The resulting structures were submitted to molecular dynamic simulations at 300 K with an integration step of 2 fs. The geometry of the water molecules was checked by the Rattle procedure (Andersen, 1983). Structures were saved every 10 ps. The atomic positions of the hydrophobic molecules (ethane) were fixed during energy minimization and simulations, but interactions were taken into account. Simulations lasting 500 ps were carried out for free Drs B2 and for the peptide adsorbed onto the hydrophobic surface.

The trajectories were analyzed in terms of root mean-square (RMS) deviations and structural parameters. The RMS deviations between the generated structures (50 structures over the 500-ps simulation) were calculated for the heavy atoms of the peptide backbone (four per amino-acid residue). These RMS deviations were used to monitor the structural conservation during simulations. The system with and without the hydrophobic support was compared by determining the number of deviations (identified as N) after three molecular simulation periods: 0–100 ps, 0–300 ps, and 0–500 ps, in each case for 2-, 3-, 4-, and 5-Å RMS deviation. The dynamical changes in the φ and ψ angles (total of 65) were also followed during 500-ps simulation and expressed as the time dependent number of angles ($\varphi + \psi$) out of the angle values ($\varphi = -57° \pm 30°$; $\psi = -47° \pm 30°$) characteristic of α-helical domain.

RESULTS AND DISCUSSION

Adsorption of dermaseptin B2 to chemically modified synthetic supports

The affinity of Drs B2 for the various self-assembled monolayers of silanes on silicon varied, and this variation was correlated with the peptide adsorption densities (Γ^m) at the saturation coverage given in Table 1. Drs B2 adsorbed most weakly to the amine-terminated SAM, and most strongly to bare silica surface. This polar surface is neutral under the experimental conditions used (pH 7.5), as the apparent pK_a of the amine surface group of the amine-terminated SAM is around pH 4 (Zhang et al., 1998). In contrast, the bare silica (pI = 2) is negatively charged at this pH. Hence, there should be an electrostatic attraction between the positively charged peptide and the negatively charged silica surface.

The average adsorption density on hydrophobic SAMs with contact angles of 92–110° was half that of the adsorption to the polar silica surface (Table 1). The adsorption of Drs B2 to these SAMs was essentially irreversible, since washing with pure buffer did not remove the adsorbed peptides. The bromo-terminated SAM gave an intermediate Γ^m value, indicating that adsorption is a hydrophobic interaction that is enhanced by Br.

Fig. 1 shows the ATR-FTIR spectra of adsorbed molecules of Drs B2 at the saturation coverage onto self-assembled monolayers of silanes on silicon. The amide I′ band centered at 1636 cm^{-1} for Drs B2 adsorbed onto the bare silica (Fig. 1 *A*, (*a*) is shifted to a higher wavenumber (around 1650 cm^{-1}) for Drs B2 adsorbed onto the hydrophobic SAMs (Fig. 1 *A*, *c*, *d*, and *e*). This shift indicates a significant change in the peptide conformation due to the

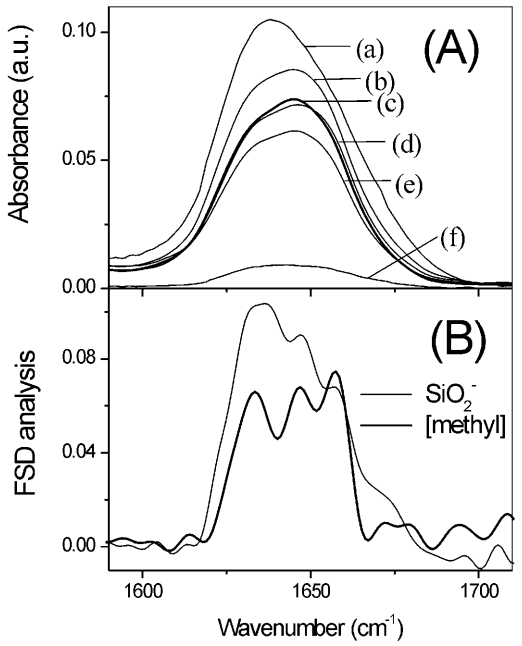

FIGURE 1 (*A*) ATR-FTIR spectra of Drs B2 (bulk concentration: 3 μM) adsorbed onto a bare silica surface *a* and onto SAMs of various compositions: *b*, [bromo]; *c*; [methyl], d; [vinyl], e; [phenyl]; and *f*, [amine]. (*B*) Fourier self-deconvolution analysis of the ATR spectra obtained for the bare silica and for the most hydrophobic surface [methyl], with an enhancement factor $k = 2$ and a bandwidth $w = 16$ cm^{-1} obtained from Omnic software.

nature of the adsorbent surfaces. FSD analysis of the ATR-FTIR spectra of adsorbed Drs B2 is shown in Fig. 1 *B*. The self-deconvolved spectrum on bare silica shows that the broad amide I′ band has two major components, one at 1635 cm^{-1} and the other at 1646 cm^{-1}. The 1635-cm^{-1} band is typical of a β-like structure, whereas the 1646 cm^{-1} band is found for deuterated random coils (Byler and Susi, 1986; Krimm and Bandekar, 1986). There are also two minor bands centered at 1656 cm^{-1} and 1673 cm^{-1}. The infrared bands around 1630–1635 cm^{-1} are generally assigned to intermolecular H-bonded carbonyls involved in β-sheets. These bonds make a 10-fold weaker contribution to the 1680–1695 cm^{-1} region (Goormaghtigh et al., 1994), which was not observed in our experiments. The large contribution at 1635 cm^{-1} and the shoulder at 1638 cm^{-1} are probably due to extended β-turns in a more or less hydrated state; they also contribute weakly to the 1675–1685 cm^{-1} region (Krimm and Bandekar, 1986; Wantyghem et al., 1990). The infrared bands near 1670–1675 cm^{-1} could also be produced by not-hydrogen bonded peptide CO in more or less polar random environments (Wantyghem et al., 1990). The infrared bands around 1652–1660 cm^{-1} are generally assigned to an α-helix (Goormaghtigh et al., 1994). The amide I′ band is composed of three components centered at 1633, 1646, and 1657 cm^{-1}, as shown in the self-deconvolved spectrum of Drs B2 adsorbed to the methyl-terminated SAM (Fig. 1 *B*). The enhancement of the spectral contribution at 1657 cm^{-1} suggests that the hydrophobic surface induces α-helical folding of the adsorbed Drs B2. Circular dichroism studies (not shown) indicate that Drs B2 adopts a random coil structure in solution in the concentration range studied.

Fig. 2 shows the densities (Γ) of Drs B2 adsorbed onto the most hydrophobic surface as a function of the bulk peptide concentration. The adsorbed peptide density increased rapidly with time at bulk concentrations of 3 μM and 1.5 μM, and reached a plateau at ~0.14 molecule/nm^2. If we consider the peptide to be a perfect α-helix spanning residues 1–33, one molecule of Drs B2 would be equivalent to a cylinder 5 nm long and 2 nm in diameter (see ''Molecular Simulation''). The cross-sectional area of one adsorbed molecule of Drs B2 would be 10 nm^2 if the molecule were horizontal to the surface and 3.14 nm^2 if it were standing on end. Hence, the theoretical Γ values of a monolayer of closed packed α-helical Drs B2 would be 0.1 (horizontal) or 0.318 molecules/nm^2 (vertical). This suggests that the experimental adsorption plateau corresponds to the formation of a dense monolayer of Drs B2 lying flat on the most hydrophobic support. At a bulk concentration of 0.3 μM, mass transport is rate limiting and the plateau is obtained only after 19 h (not shown). The time-dependent adsorption densities obtained on the bare silica are shown in Fig. 2. The twofold increase in the adsorption plateau could be due to the formation of a bilayer of Drs B2 in a pure α-helical conformation. But the FTIR analysis gives a higher fraction of β-like structure in the adsorbed peptides at saturation of the bare silica support, which prevents any speculation about the cross-sectional area occupied by the adsorbed peptide. It is not possible to conclude whether the adsorption plateau corresponds to the formation of a densely packed monolayer of Drs B2 in an average given conformation or to loosely packed multiple layers.

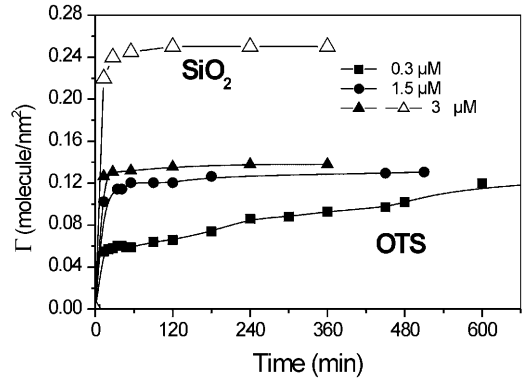

FIGURE 2 Kinetics of Drs B2 adsorption onto the hydrophobic surface [methyl] at increasing bulk peptide concentrations (0.3, 1.5, and 3 μM) and onto bare silica at 3 μM, measured under stationary conditions by ATR-FTIR.

Adsorption kinetics in flow experiments by SPR

The SPR response (a change in resonance signal), expressed as response units (RU), depends both on the bulk dermaseptin concentration and the surface of the sensor chip (Fig. 3). The correlation between RU and adsorbed mass is ~1000 RU for 1 ng molecules/mm^2 (Stenberg et al., 1991). The calculated surface density for a compact monolayer of Drs B2 is 0.54 ng/mm^2, which corresponds to ~650 RU (1.2 mm^2 for detection). The monolayer coverage of the hydrophobic HPA sensor chip is not complete after 180 s of adsorption at bulk peptide concentrations lower than 5 μM, and the adsorbed peptide is irreversibly immobilized on the methylated support. Relative responses at the adsorption plateau were 720 $\pm$ 20 RU at higher bulk peptide concentration, corresponding to a monolayer coverage of the surface (Fig. 3 *A*). The nonspecific interaction between the peptide and the methylated support is governed by a surface-limited rate. Most of the adsorbed peptides cannot be desorbed, as shown by ATR-FTIR experiments. The preferred orientation of adsorbed Drs B2 molecules near the jamming limit, which places its external hydrophobic surface toward the hydrophobic support, will increase the electrostatic repulsion between the positive charges of the bound peptide and those of free Drs B2. A second monomolecular layer of Drs B2 cannot be formed, as confirmed by the ATR-FTIR results (Fig. 2).

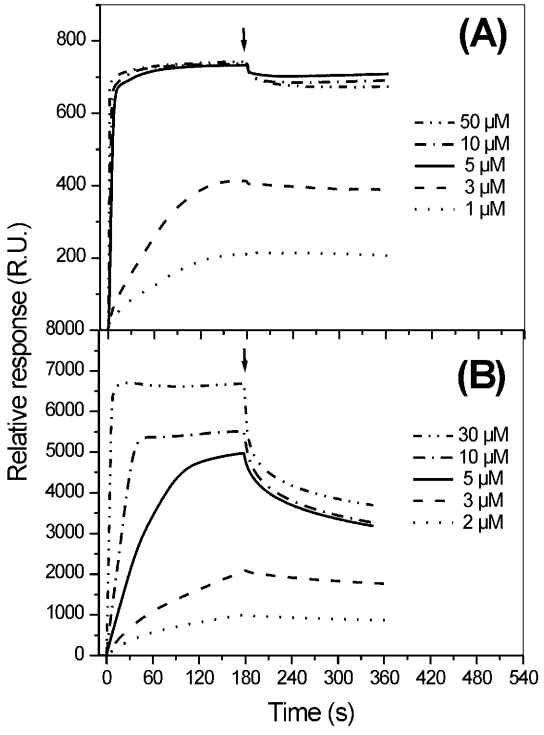

FIGURE 3 SPR study at various bulk concentrations on the adsorption/desorption of Drs B2 onto (*A*) a hydrophobic (HPA) surface, and (*B*) a hydrophilic (CM5) surface. The arrow indicates the start of desorption.

The relative responses reached 2000 RU for the hydrophilic CM5 sensor chip and bulk peptide concentrations below 5 μM. This approximates the adsorption densities obtained on bare silica by ATR-FTIR experiments (Fig. 3 *B*). This layer is not desorbed by rinsing. The peptide molecules are stacked to give a density of 7200 RU at bulk peptide concentrations >5 μM. This corresponds to the formation of multiple layers, but the final relative response is 2000 RU after 30 min of desorption. However, there are weakly adsorbed multiple layers on CM5. The BIAcore specification indicates that the CM5 sensor chip has a nonplanar surface that could increase the adsorption density, with the possibility of peptides penetrating into the gel (Hall, 2001).

Nonlinear curve fitting of the layouts was attempted with theoretical models described in the BIAevaluation software (see ''Materials and Methods''). However, no satisfactory solutions were found that corresponded to the nonspecific adsorption shown in this study. A recent review describes the difficulties encountered when simulating biosensorgrams with Langmuir-type models and discusses the causes of the nonideal cases, including conformational changes and multiple binding sites (Hall, 2001). The development of an exact analytical formulation taking into account the geometry and charges of the adsorbed macromolecules is still under way. Simulation of our data with such models is beyond the scope of this paper, but readers may refer to several theoretical studies (Fang and Szleifer, 2001; Van Tassel et al., 1994), in which the complex adsorption kinetics of biomolecules to planar synthetic supports are discussed.

Conformational changes during the adsorption of Drs B2 onto a hydrophobic support

Fig. 4 shows the synchronous and asynchronous 2D maps for one-dimensional ATR-FTIR spectra of Drs B2 adsorbed at a concentration of 0.3 μM onto the methyl-terminated SAM. There are three major auto peaks on the diagonal of the S-map, at 1618, 1655, and 1675 cm^{-1}. The auto peak at 1618 cm^{-1} can be assigned to intermolecular hydrogen-bonded peptide carbonyls involved in self-association (Dwivedi and Krimm, 1984). This component band is not present on the self-deconvolved ATR spectrum for saturation coverage of the hydrophobic surface [methyl] by Drs B2 (Fig. 1 *B*). Whereas the band component at 1618 cm^{-1} is present in spectra recorded at the beginning of the adsorption process, it has disappeared once the peptide monolayer is complete (data not shown). The positive crosspeak at (1618, 1675) cm^{-1} indicates that the intensity changes correlated by this pair of wavenumbers are either increasing or decreasing together with respect to the time-dependent adsorption. Negative crosspeaks at (1618, 1655) and (1655, 1675) cm^{-1} suggest that the intensity of the component band centered at 1655 cm^{-1} increases with time, whereas the intensities at

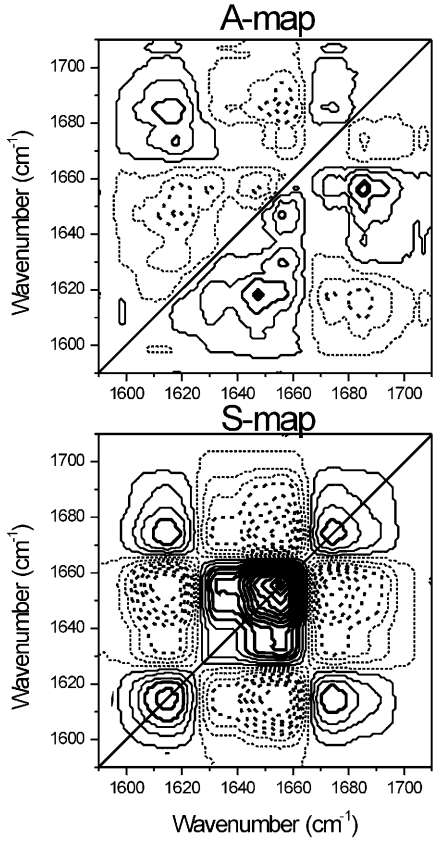

FIGURE 4 2D-correlation S-map and A-map of Drs B2 (0.3 μM) adsorbed onto a hydrophobic surface [methyl] constructed from time-dependent ATR spectra in the amide I′ band spectral region. Negative crosspeaks are shown by dot-dashed lines and positive ones by solid lines.

1618 cm^{-1} and 1675 cm^{-1} decrease. In other words, the α-helical folding increases during adsorption at the expense of self-association (1618 cm^{-1}) and turns (1675 cm^{-1}).

The corresponding A-map shows a number of peaks whose positions are slightly different from those detected by the S-map (Fig. 4). This has been observed by others (Czarnik-Matusewicz et al., 2000; Gericke et al., 1996). Because the A-map is more sensitive to variations in the intensity of one-dimensional spectra than is the S-map, the peaks at 1630, 1647, and 1685 cm^{-1} are not well defined in the corresponding S-map. We will discuss only the crosspeaks present on both the S- and A-maps. The A-map for the adsorption-dependent changes (Fig. 4) reveals that crosspeaks at (1618, 1655) cm^{-1} are negative and correspond to negative crosspeaks on the S-map, so that the change in the component at 1618 cm^{-1} is in advance with respect to the correlated IR component at 1655 cm^{-1} (see details in ''Materials and Methods''). This indicates that the self-associated domains should disappear before the folding of the α-helix takes place. The crosspeak at (1655, 1675) cm^{-1} is negative on both the A-map and the S-map, so that the folding of the α-helix occurs before the unfolding of turns.

Orientation of the Drs B2 at the ^2H_2O/hydrophobic interface

The polarized ATR spectra and curve-fitted spectra of the complete monolayer of Drs B2 adsorbed onto the [methyl] surface are shown in Fig. 5. The component band at 1657 cm^{-1} attributed to α-helix structure reflects a large difference in absorption intensity after the polarization of the infrared beam. The component band at 1632 cm^{-1} has similar intensities in both polarizations, whereas the component band at 1645 cm^{-1} is slightly shifted to 1647 cm^{-1} in the perpendicular polarization. The dichroic ratio of the characteristic α-helix vibrational mode at 1657 cm^{-1} was 1.62 $\pm$ 0.05, which corresponds to an order parameter S_m of -0.394 ± 0.07, which leads to an average tilt angle of 75 $\pm$ 5° for the peptide helix with the normal to pure hydrophobic surface.

We measured the dichroic ratio at the air/hydrophobic interface by drying the monolayer of Drs B2. Changing the bulk phase from deuterated water to air changed the amide I band, so that it had only a single major component band

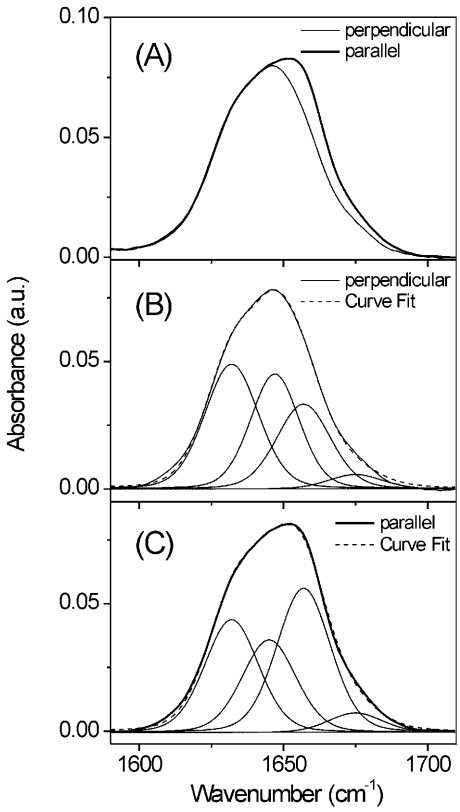

FIGURE 5 Polarized ATR-FTIR spectra of a complete monolayer of Drs B2 adsorbed at the ^2H_2O/hydrophobic interface (*top*); spectral decomposition of the amide I′ band for the perpendicular polarization (*middle*) and for the parallel polarization (*bottom*). The component bands are the results of the curve fitting using the wavenumbers of the components set at 1633, 1646, 1657, and 1673 cm^{-1} deduced from the FSD analysis (see Fig.1 *B*). The Lorentzian/Gaussian profile was set at 0.25 and the bandwidth of the components at 22 cm^{-1}. The best-average fit gave the intensity of each component band for each spectrum.

centered at 1652 cm^{-1} (spectra not shown). The dichroic ratio at this wavenumber is 1.58 ± 0.05, indicating that the peptide is orientated parallel to the hydrophobic surface ($S_m = -0.5$). The air phase could contribute to a more hydrophobic environment for the Drs B2, which could make the α-helix more stable, with a nearly perfect orientation. Hydration plays a major role in the orientation of peptides in lipid bilayers. For example, melittin has a very different orientation when embedded in a hydrated phospholipid bilayer than when it is in a dry one (Frey and Tamm, 1991).

Molecular simulations

Qualitatively, the higher root mean-square deviation (rmsd) parameters (N) indicate that structures have a longer average lifetime in the presence of the hydrophobic surface (Table 2). The quantitative ratio $N_{\text{with plate}}/N_{\text{without plate}}$ indicates that differences with and without the hydrophobic plate are the most significant below rmsd 5 Å and for the longer simulation period. Only short helical domains are stable for rmsd correlations corresponding to 3 and 4 Å. The averaged $N_{\text{with plate}}/N_{\text{without plate}}$ ratios of 1.2 for the 0–100 ps period, 1.3 for the 0–300 ps period, and 2.1 for the 0–500 ps period indicate that there is very little difference between the two systems early in simulation, but that the difference increases with time. These results are well corroborated by the time-dependent change in the number of backbone angles ($\varphi + \psi$) out of α-helix domain (Fig. 6). During a first step ($t < 200$ ps), with and without the plate, ~12 residues out of 33 (~24 angles over 65) leave the initial α-helix. Then ~8 additional residues become unfolded without the hydrophobic support during the second step ($t > 200$ ps), whereas only ~2 residues become unfolded with the support. If we assume that the transition from α-helix to disordered state is a first-order process, the data in Fig. 6 can be parameterized as $(A - 1) = a \times [1 - \exp(-bt)]$, where A is the total number of angles, $a + 1$ is the time-dependent number of angles out of α helix, and b is the rate constant required to remove one residue from the initial α-helix domain. Thus the fitted results give 49 angles of the initial α-helix for free Drs B2, and only 33 for the system with the hydrophobic support. Only ~8 residues of the 33 residues are involved in the helical domains in an aqueous medium, whereas 16 residues are part of the helical structure when the peptide is on a hydrophobic support.

TABLE 2 Total number of correlations as a function of the RMS deviations level for systems with and without the hydrophobic support

		2 Å	3 Å	4 Å	5 Å
0–100 ps	$N_{\text{without plate}}$	15	33	42	45*
	$N_{\text{with plate}}$	16	45*	45*	45*
	$N_{\text{with plate}}/N_{\text{without plate}}$	1.07	1.36	1.07	1.00
0–300 ps	$N_{\text{without plate}}$	45	130	243	409
	$N_{\text{with plate}}$	57	172	306	404
	$N_{\text{with plate}}/N_{\text{without plate}}$	1.27	1.32	1.26	0.99
0–500 ps	$N_{\text{without plate}}$	59	191	386	745
	$N_{\text{with plate}}$	183	447	734	1090
	$N_{\text{with plate}}/N_{\text{without plate}}$	3.1	2.34	1.9	1.46

*Indicates a maximum number of correlations.

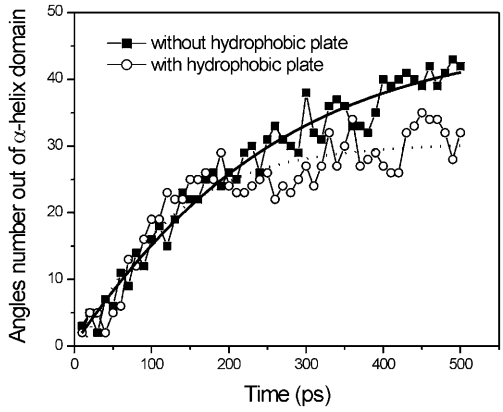

FIGURE 6 Total number of φ and ψ angles out of the α-helix domain during the simulation time, for Drs B2 in aqueous medium and for the system Drs B2 with hydrophobic support.

More detailed information can be obtained on individual angles along the polypeptide chain. The angles that show few residues outside the α-helix domain, i.e., below 12/50, were identified during the 500-ps molecular simulation. We have considered an α-helix sequence to be stable if at least three consecutive angles fit with the α-helix geometry. Three similar domains appear to be preserved from unfolding in both systems: ψ5–ψ9, ψ16–φ18, and ψ29–φ30 without the hydrophobic support, and ψ4–ψ7, ψ15–ψ17, and φ28–ψ30 with the hydrophobic support (Fig. 7). Two other domains are protected only in the presence of the hydrophobic support (φ19–ψ21 and φ23–ψ24). The gain in helical structure involves mainly lysine and alanine residues. The peptide domain closest to the hydrophobic plate involves Ala-14, Ala-16, Ala-17, and Ala-18, whereas Lys-11, Lys-15, and Lys-19 are outside the plate (Fig. 8). The short Lys-19–Ala-21 and Lys-23–Ala-25 folding in the presence of the hydrophobic surface could favor the partitioning of the residues, with the hydrophobic residues being toward the hydrophobic plate and the charged lysine side chain toward the aqueous medium. This is in close agreement with several calculations recently performed on alanine-rich peptides with lysine residues. The main results indicate that ionizable lysine residues in a sequence sequester the water away from the CO and NH groups of the backbone, thus enabling them to form internal hydrogen bonds (Groebke et al., 1996; Sung, 1995; Vila et al., 2000, 1998). This solvation effect dictates the conformation, and hence modifies the conformational propensity of alanine residues to stabilize the α-helix. These

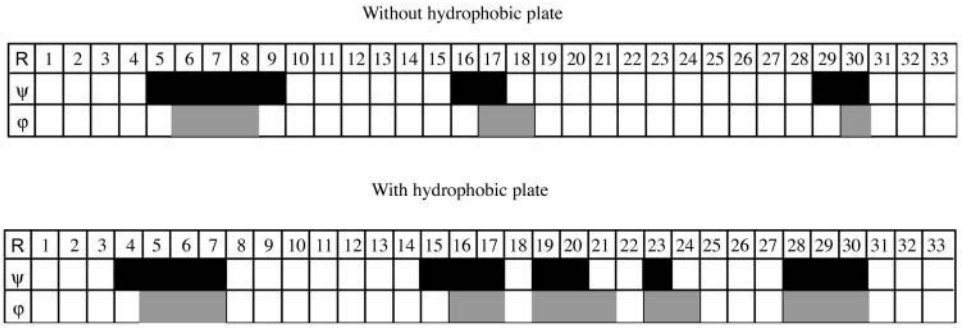

FIGURE 7 Low exit frequencies from α-helix domain for the free Drs B2 or Drs B2 adsorbed onto a hydrophobic support.

helix propensities depend strongly on the lysine content (Williams et al., 1998).

Previous molecular dynamics studies of peptide/lipid bilayer interactions have shown that dermaseptin B1 is more stabilized by the mean field potential of a lipid bilayer than with a pure hydrophobic potential (La Rocca et al., 1999). These authors also observed that the more stabilized structure in an all-atoms simulation of a Drs B1/bilayer system was an α-helix oriented with its external polar surface toward the aqueous medium and its nonpolar surface toward the bilayer. Finally, the hydrophobic support does not seem to completely protect an extended α-helix Drs B2 structure.

CONCLUSION

The adsorption of peptides at aqueous/solid interface depends on the specificity of the interactions, and these can readily be studied by ATR and SPR using easily compared synthetic solid supports. Electrostatic interaction leads to the irreversible adsorption of a layer in which most of the peptide molecules have an extended β-like conformation. Hydrophobic interaction leads to the irreversible adsorption of one monolayer of Drs B2 molecules in an α-helical conformation. The orientation of the α-helical peptide molecules has been determined by polarized ATR and confirmed by molecular dynamics. The hydrophobic residues such as alanine are oriented toward the hydrophobic support and the positively charged lysine residues face the aqueous medium to maintain an α-helical conformation in the adsorbed state as in solution. The C-terminal region of Drs B2 is rich in lysine and leads to the peptide molecules being tilted with respect to the support. The affinity of Drs B2 for the hydrophobic support is so great that the gradual α-helix folding can only be observed in conditions of limitation of mass transport by ATR-FTIR. 2D correlation analysis revealed the influence of peptide-peptide compaction on the promotion of α-helix conformation in the adsorbed monolayer.

The surface-adsorbed dermaseptin adopts a different specific conformation whether the planar support is hydrophilic or hydrophobic. By forming α-helical structure on hydrophobic supports, the solvent-exposed helical face, which is rich in lysine residues, can also be used for further chemical linkages or for controlled electrostatic properties. These specific secondary structures as well as the orientation of the amphipathic peptides on solid supports provide directions for the development of peptide coatings for designed biomaterials.

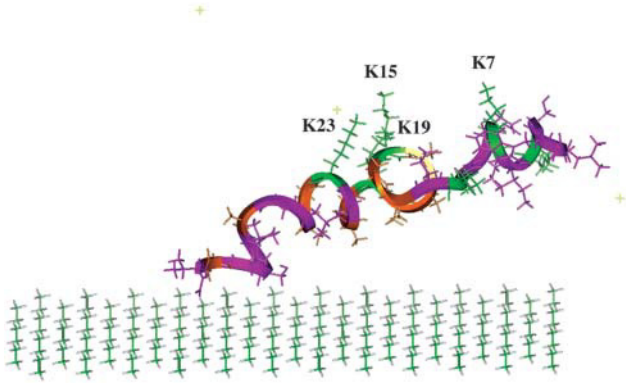

FIGURE 8 Snapshot of the molecular dynamics simulation of the Drs B2 bound to the hydrophobic support at 500 ps. The Ala residues are in orange and the Lys residues are in green.

The authors are grateful to the Service de Modélisation et Imagerie Moleculaires of the Réseau Fédératif de Recherche of the University of Paris VI for calculation facilitations.

REFERENCES

Andersen, H. C. 1983. Rattle: a velocity version of shake algorithm for molecular dynamics calculations. *J. Comput. Physics*. 52:24–34.

Axelsen, P. H., and M. J. Citra. 1996. Orientational order determination by internal reflection infrared spectroscopy. *Prog. Biophys. Mol. Biol.* 66: 227–253.

Balachander, N., and C. N. Sukenik. 1990. Monolayer transformation by nucleophilic substitutions to the creation of new monolayer assemblies. *Langmuir*. 6:1621–1627.

Bower, C. K., J. McGuire, and M. A. Daeschel. 1995. Influences on the antimicrobial activity of surface-adsorbed nisin. *J. Ind. Microbiol.* 15:227–233.

Brand, G. D., J. R. Leite, L. P. Silva, S. Albuquerque, M. V. Prates, R. B. Azevedo, V. Carregaro, J. S. Da Silva, V. C. Sa, R. A. Brandao, and C.

Block, Jr. 2002. Dermaseptins from Phyllomedusa oreades and Phyllomedusa distincta: Anti-Trypanosoma cruzi activity without cytotoxicity to mammalian cells. *J. Biol. Chem.* 277:49332–49340.

Byler, D. M., and H. Susi. 1986. Examination of the secondary structure of proteins by deconvolved FTIR spectra. *Biopolymers.* 25:469–487.

Castano, S., B. Desbat, M. Laguerre, and J. Dufourcq. 1999. Structure, orientation and affinity for interfaces and lipids of ideally amphipathic lytic LiKj(i=2j) peptides. *Biochim. Biophys. Acta.* 1416:176–194.

Charpentier, S., M. Amiche, J. Mester, V. Vouille, J. P. Le Caer, P. Nicolas, and A. Delfour. 1998. Structure, synthesis, and molecular cloning of dermaseptins B, a family of skin peptide antibiotics. *J. Biol. Chem.* 273:14690–14697.

Citra, M. J., and P. H. Axelsen. 1996. Determination of molecular order in supported lipid membranes by internal reflection Fourier transform infrared spectroscopy. *Biophys. J.* 71:1796–1805.

Cooper, M. A., A. C. Try, J. Carroll, D. J. Ellar, and D. H. Williams. 1998. Surface plasmon resonance analysis at a supported lipid monolayer. *Biochim. Biophys. Acta.* 1373:101–111.

Czarnik-Matusewicz, B., K. Murayama, Y. Q. Wu, and Y. Ozaki. 2000. Two-dimensional attenuated total reflection/infrared correlation spectroscopy of adsorption-induced and concentration-dependent spectral variations of beta-lactoglobulin in aqueous solutions. *J. Phys. Chem. B.* 104:7803–7811.

Daly, J. W., J. Caceres, R. W. Moni, F. Gusovsky, M. Moos, Jr., K. B. Seamon, K. Milton, and C. W. Myers. 1992. Frog secretions and hunting magic in the upper Amazon: identification of a peptide that interacts with an adenosine receptor. *Proc. Natl. Acad. Sci. USA.* 89:10960–10963.

Dwivedi, A. M., and S. Krimm. 1984. Vibrational analysis of peptides, polypeptides, and proteins. XVIII. Conformational sensitivity of the α-helix spectrum: αI- and αII-poly(L-alanine). *Biopolymers.* 23:923–943.

Fabian, H., H. H. Mantsch, and C. P. Schultz. 1999. Two-dimensional IR correlation spectroscopy: sequential events in the unfolding process of the lambda cro-V55C repressor protein. *Proc. Natl. Acad. Sci. USA.* 96:13153–13158.

Fang, F., and I. Szleifer. 2001. Kinetics and Thermodynamics of Protein Adsorption: A Generalized Molecular Theoretical Approach. *Biophys. J.* 80:2568–2589.

Feder, R., A. Dagan, and A. Mor. 2000. Structure-activity relationship study of antimicrobial dermaseptin S4 showing the consequences of peptide oligomerization on selective cytotoxicity. *J. Biol. Chem.* 275: 4230–4238.

Fleury, Y., M. A. Dayem, J. J. Montagne, E. Chaboisseau, J. P. Le Caer, P. Nicolas, and A. Delfour. 1996. Covalent structure, synthesis, and structure-function studies of mesentericin Y 105(37), a defensive peptide from gram-positive bacteria Leuconostoc mesenteroides. *J. Biol. Chem.* 271:14421–14429.

Frey, S., and L. K. Tamm. 1991. Orientation of melittin in phospholipid bilayers. A polarized attenuated total reflection infrared study. *Biophys. J.* 60:922–930.

Gericke, A., S. J. Gadaleta, J. W. Brauner, and R. Mendelsohn. 1996. Characterization of biological samples by two-dimensional infrared spectroscopy: simulation of frequency, bandwith, and intensity changes. *Biospectroscopy.* 2:341–351.

Goormaghtigh, E., V. Cabiaux, and J. M. Ruysschaert. 1994. Determination of soluble and membrane protein structure by Fourier Transform Infrared spectroscopy. I. Assignments and model compounds. *In* Subcellular Biochemistry. H. J. Hiderson and G. B. Ralston, editors. Plenum Press, New York. 329–362.

Goormaghtigh, E., and J.-M. Ruysschaert. 1990. Polarized ATR infrared spectroscopy as a tool to investigate the conformation and orientation of membrane components. *In* Molecular Description of Biological Membranes by Computer Aided Conformational Analysis. R. Brasseur, editor. CRC Press, Boca Raton, FL. 285–329.

Groebke, K., P. Renold, K. Y. Tsang, T. J. Allen, K. F. McClure, and D. S. Kemp. 1996. Template-nucleated alanine-lysine helices are stabilized by position-dependent interactions between the lysine side chain and the helix barrel. *Proc. Natl. Acad. Sci. USA.* 93:4025–4029.

Hagler, A. T., P. S. Stren, R. Sharon, J. M. Becker, and F. Naider. 1979. Computer simulation of the conformational properties of oligopeptides. Comparison of theoretical methods and analysis of experimental results. *J. Am. Chem. Soc.* 101:6842–6852.

Hall, D. 2001. Use of optical biosensors for the study of mechanistically concerted surface adsorption processes. *Anal. Biochem.* 288:109–125.

Harrick, N. J. 1967. INTERNAL REFLECTION SPECTROSCOPY. Interscience, New York.

Harvey, L. J., G. Bloomberg, and D. C. Clark. 1995. The influence of surface hydrophobicity on the adsorbed conformation of a β-sheet-forming synthetic peptide. *J. Colloid Interface Sci.* 170:161–168.

Hlady, V., and J. Buijs. 1996. Protein adsorption on solid surfaces. *Curr. Opin. Biotechnol.* 7:72–77.

Krimm, S., and J. Bandekar. 1986. Vibrational spectroscopy and conformation of peptides, polypeptides, and proteins. *Adv. Protein Chem.* 38:181–364.

Kumary, V. K., and R. Nagaraj. 2001. Structure-function studies on the amphibian peptide brevinin 1E: translocating the cationic segment from the C-terminal end to a central position favors selective antibacterial activity. *J. Pept. Res.* 58:433–441.

Kustanovich, I., D. E. Shalev, M. Mikhlin, L. Gaidukov, and A. Mor. 2002. Structural requirements for potent versus selective cytotoxicity for antimicrobial dermaseptin S4 derivatives. *J. Biol. Chem.* 277:16941–16951.

Kwon, M. Y., S. Y. Hong, and K. H. Lee. 1998. Structure-activity analysis of brevinin 1E amide, an antimicrobial peptide from Rana esculenta. *Biochim. Biophys. Acta.* 1387:239–248.

La Rocca, P., P. C. Biggin, D. P. Tieleman, and M. S. Sansom. 1999. Simulation studies of the interaction of antimicrobial peptides and lipid bilayers. *Biochim. Biophys. Acta.* 1462:185–200.

Laczko, I., M. Hollosi, L. Urge, K. E. Ugen, D. B. Weiner, H. H. Mantsch, J. Thurin, and L. Otvos, Jr. 1992. Synthesis and conformational studies of N-glycosylated analogues of the HIV-1 principal neutralizing determinant. *Biochemistry.* 31:4282–4288.

Lecomte, S., C. Hilleriteau, J. P. Forgerit, M. Revault, M. H. Baron, P. Hildebrandt, and T. Soulimane. 2001. Structural changes of cytochrome c(552) from Thermus thermophilus adsorbed on anionic and hydrophobic surfaces probed by FTIR and 2D-FTIR spectroscopy. *Chembiochem.* 2:180–189.

Lee, D. G., P. I. Kim, Y. Park, E. R. Woo, J. S. Choi, C. H. Choi, and K. S. Hahm. 2002. Design of novel peptide analogs with potent fungicidal activity, based on PMAP-23 antimicrobial peptide isolated from porcine myeloid. *Biochem. Biophys. Res. Commun.* 293:231–238.

Lewis, R. N., E. J. Prenner, L. H. Kondejewski, C. R. Flach, R. Mendelsohn, R. S. Hodges, and R. N. McElhaney. 1999. Fourier transform infrared spectroscopic studies of the interaction of the antimicrobial peptide gramicidin S with lipid micelles and with lipid monolayer and bilayer membranes. *Biochemistry.* 38:15193–15203.

Long, J. R., N. Oyler, G. P. Drobny, and P. S. Stayton. 2002. Assembly of α-helical peptide coatings on hydrophobic surfaces. *J. Am. Chem. Soc.* 124:6297–6303.

Losset, D., G. Dupas, J. Duflos, J. Bourguignon, and G. Queguiner. 1991. Induction asymetrique supramoleculaire par un reactif modele du NADH greffe sur silice. *Bull. Soc. Chim. Fr.* 128:721–729.

Maget-Dana, R. 1999. The monolayer technique: a potent tool for studying the interfacial properties of antimicrobial and membrane-lytic peptides and their interactions with lipid membranes. *Biochim. Biophys. Acta.* 1462:109–140.

Marsh, D., M. Müller, and F.-J. Schmidt. 2000. Orientation of the Infrared transition moments for an α-helix. *Biophys. J.* 78:2499–2510.

Matsuzaki, K., K. Sugishita, N. Ishibe, M. Ueha, S. Nakata, K. Miyajima, and R. M. Epand. 1998. Relationship of membrane curvature to the formation of pores by magainin 2. *Biochemistry.* 37:11856–11863.

Meskers, S., J.-M. Ruysschaert, and E. Goormaghtigh. 1999. H-D exchange of streptavidin and its complex with biotin studied by 2D ATR FTIR spectroscopy. *J. Am. Chem. Soc.* 121:5115–5122.

Mor, A., M. Amiche, and P. Nicolas. 1994a. Structure, synthesis, and activity of dermaseptin *b*, a novel vertebrate defensive peptide from frog skin: relationships with adenoregulin. *Biochemistry*. 33:6642–6650.

Mor, A., K. Hani, and P. Nicolas. 1994b. The vertebrate peptide antibiotics dermaseptins have overlapping structural features but target specific microorganisms. *J. Biol. Chem.* 269:31635–31641.

Mrksich, M., G. B. Sigal, and G. M. Whitesides. 1995. Surface plasmon resonance permits in situ measurement of protein adsorption on self-assembled monolayers of alkanethiolates on gold. *Langmuir*. 11:4383–4385.

Nicolas, P., and A. Mor. 1995. Peptides as weapons against microorganisms in the chemical defense system of vertebrates. *Annu. Rev. Microbiol.* 49:277–304.

Noda, I. 1990. Two-dimensional infrared (2D IR) spectroscopy: theory and applications. *Appl. Spectrosc.* 44:550–561.

Noinville, S., M. Revault, M.-H. Baron, A. Tiss, S. Yapoudjian, M. Ivanova, and R. Verger. 2002. Conformational changes and orientation of Humicola lanuginosa lipase on a solid hydrophobic surface: an in situ interface FTIR-ATR study. *Biophys. J.* 82:2709–2719.

Noinville, V., C. Vidal-Madjar, and B. Sébille. 1995. Modeling of protein adsorption on polymer surfaces. Computation of adsorption potential. *J. Phys. Chem.* 99:1516–1522.

Norde, W. 2000. Proteins at solid surfaces. *In* Physical Chemistry of Biological Interfaces. A. Baszkin and W. Norde, editors. Marcel Dekker, New York. 115–136.

Park, S., S. H. Park, H. C. Ahn, S. Kim, S. S. Kim, and B. J. Lee. 2001. Structural study of novel antimicrobial peptides, nigrocins, isolated from Rana nigromaculata. *FEBS Lett.* 507:95–100.

Ramsden, J. J. 1998. Kinetics of Protein Adsorption. Biopolymers at Interfaces. Marcel Dekker, New York. 321–361.

Schweizer, E. E., W. S. Creasy, K. K. Light, and E. T. Shaffer. 1969. Reactions of phosphorous compounds. XX. Reactions of furfuryl-, dihydrofurfuryl-, and tetrahydrofurfuryltriphenylphosphonium bromide. *J. Org. Chem.* 34:212–216.

Shai, Y. 1999. Mechanism of the binding, insertion and destabilization of phospholipid bilayer membranes by alpha-helical antimicrobial and cell non-selective membrane-lytic peptides. *Biochim. Biophys. Acta*. 1462:55–70.

Smeller, L., and K. Heremans. 1999. 2D FT-IR spectroscopy analysis of the pressure-induced changes in proteins. *Vibrational Spectroscopy*. 19:375–378.

Stenberg, E., B. Persson, H. Roos, and C. Urbaniczsky. 1991. Quantitative determination of surface concentration of protein with surface plasmon resonance using radiolabeled proteins. *J. Colloid Interface Sci.* 143:513–526.

Strahilevitz, J., A. Mor, P. Nicolas, and Y. Shai. 1994. Spectrum of antimicrobial activity and assembly of dermaseptin-b and its precursor form in phospholipid membranes. *Biochemistry*. 33:10951–10960.

Sung, S. S. 1995. Folding simulations of alanine-based peptides with lysine residues. *Biophys. J.* 68:826–834.

Van Tassel, P. R., P. Viot, G. Tarjus, and J. Talbot. 1994. Irreversible adsorption of macromolecules at a liquid-solid interface: theoretical studies of the effects of conformational change. *J. Chem. Phys.* 101: 7064–7073.

Vila, J. A., D. R. Ripoll, and H. A. Scheraga. 2000. Physical reasons for the unusual alpha-helix stabilization afforded by charged or neutral polar residues in alanine-rich peptides. *Proc. Natl. Acad. Sci. USA*. 97:13075–13079.

Vila, J. A., D. R. Ripoll, M. E. Villegas, Y. N. Vorobjev, and H. A. Scheraga. 1998. Role of hydrophobicity and solvent-mediated charge-charge interactions in stabilizing alpha-helices. *Biophys. J.* 75:2637–2646.

Wade, D., J. Silberring, R. Soliymani, S. Heikkinen, I. Kilpelainen, H. Lankinen, and P. Kuusela. 2000. Antibacterial activities of temporin A analogs. *FEBS Lett.* 479:6–9.

Wantyghem, J., M.-H. Baron, M. Picquart, and F. Lavialle. 1990. Conformational changes of Robinia pseudoacacia Lectin related to modifications of the environment: FTIR investigation. *Biochemistry*. 29:6600–6609.

Wasserman, S. R., G. M. Whitesides, I. M. Tidswell, B. M. Ocko, P. S. Pershan, and J. D. Axe. 1989. The structure of self-assembled monolayers of alkylsiloxanes on silicon: a comparison of results from ellipsometry and low-angle X-ray reflectivity. *J. Am. Chem. Soc.* 111:5852–5861.

Whitesides, G. M., and P. E. Laibinis. 1990. Wet chemical approaches to the characterization of organic surfaces: self-assembled monolayers, wetting, and the physical-organic-chemistry of the solid-liquid interface. *Langmuir*. 6:87–96.

Williams, L. W., K. Kather, and D. S. Kemp. 1998. High helicities of Lys-containing, Ala-rich peptides are primarily attributable to a large, context-dependent Lys stabilization. *J. Am. Chem. Soc.* 120:11033–11043.

Zhang, H., H.-X. He, J. Wang, T. Mu, and Z.-F. Liu. 1998. Force titration of amino group-terminated self-assembled monolayers using chemical force microscopy. *Appl. Phys. A*. 66:S269–S271.